N73-17722

Interior Radiances in Optically Deep Absorbing Media

II. Rayleigh Scattering

by

Gilbert N. Plass, George W. Kattawar, and Judith Binstock

Report No. 6

The research described in this report was

funded by the

National Aeronautics and Space Administration

Contract No. NGR 44-001-117

Department of Physics
Texas A&M University
College Station, Texas 77843

January 3, 1973

A paper based on the material in this report has been submitted to the Journal of Quantitative Spectroscopy and Radiative Transfer.

Page Intentionally Left Blank

Interior Radiances in Optically Deep Absorbing Media

II. Rayleigh Scattering

Gilbert N. Plass, George W. Kattawar, and Judith Binstock

Department of Physics, Texas A&M University

College Station, Texas 77843

ABSTRACT

The interior radiances are calculated within an optically deep absorbing medium scattering according to the Rayleigh phase function. The accuracy of the matrix operator method is improved by many orders of magnitude through the use of accurate starting values obtained by the Runge-Kutta method rather than from the single scattering approximation. The radiance and flux are given for a range of solar zenith angles and for single scattering albedos of 1, 0.99, 0.9, 0.5, and 0.1. The development of the asymptotic angular distribution of the radiance is illustrated. It is shown that this asymptotic distribution is probably physically unobservable when $\omega_o<0.8$, since the flux is less than 10^{-8} of its original value at the beginning of the asymptotic region. The ratio of the upward to downward flux is calculated and is shown to be remarkably constant within the medium except very close to the boundaries. The heating rate within the medium is found to be very nearly proportional to the downward flux, except near the boundaries. When the single scattering albedo is small, a number of examples illustrate the significant contribution of the direct solar flux to the total flux even at great optical depths within the medium. The total downward flux decreases exponentially with optical depth away from boundaries when the single scattering albedo is greater than or equal to 0.9; when it is less than or equal to 0.5 only an approximate exponential fit can be obtained within the region accessible to experimental observation.

INTRODUCTION

Results are given in this paper for the interior radiance within optically deep absorbing clouds and its dependence on the single scattering albedo and the optical depth within the cloud. The matrix operator theory recently reviewed by Plass, Kattawar, and Catchings[1] is used to obtain an entirely rigorous numerical solution of the radiative transfer equations. The Rayleigh phase function is used for illustration in these first calculations, although the method is applicable to general phase functions. Further details of the matrix operator method are given in the first part of this paper by Kattawar and Plass[2] (hereafter referred to as I). A starting proceedure which uses the Runge-Kutta method instead of the usual single scattering approximation improves the accuracy by many orders of magnitude in typical cases as described in I. A detailed discussion of errors in a one-dimensional matrix operator calculation is presented in I; in most cases these results apply equally well to the multidirectional case.

Interior radiances can casily be calculated by Monte Carlo methods. Results obtained in this manner have been reported by Plass and Kattawar[3,4] and Kattawar and Plass[5]. Interior radiances were obtained at points within the earth's ocean-atmosphere system. These appear to be the only reasonably accurate values for the interior radiance which have been reported in the literature. A relatively simple equation for the interior radiances originally given by Bellman[6] (see equations (3-4) on p. 348) and based on the matrix operator theory does not appear to have been used previously in practical calculations.

The results given here show the dependence of the interior radiance

and flux on the optical depth within the medium as well as on its absorbing and scattering properties. The development of the asymtotic angular distribution of the radiance is illustrated. This asymptotic distribution is unobservable when the single scattering albedo is small, since the region only begins at great optical depths where the flux is extremely small. The range of optical depth for which the ratio of the upward to downward flux is constant is investiaged as is the region in which the decrease of the downward flux with optical depth can be represented by an exponential. The heating rate within the medium is calculated and found to be nearly proportional to the downward flux except near boundaries.

DOWNWARD RADIANCE

The interior radiances were calculated from Equations (5) and (6) of Plass, Kattawar, and Catchings[1] by the methods of matrix operator theory as reviewed by them. Greatly improved accuracy was obtained by the use of a Runge-Kutta method to obtain a starting value instead of using the single scattering approximation. The differential equations satisfied by the reflection and transmission operators (see Kattawar[7]) were integrated from the origin to an optical depth of the order of 10^{-3}. Since the error of the Runge-Kutta method is proportional to h^5 where h is the interval size, the solution at this optical depth has an error of the order of 10^{-15}. This is approximately equivalent to machine accuracy since all calculations reported here were done in double precision on the IBM 360/65 (the equivalent of 16 significant figures). Each of the five cases reported here required approximately 4 minutes of computer time.

The calculations were continued out to very large (τ = 16,794) optical depths when the single scattering albedo $\omega_o = 1$; when $\omega_o < 1$ the

calculations were carried out to optical depths of 45 to 109 depending on the particular value of ω_o. In each case results were calculated for several different values for the albedo of the lower surface. However, this is not of particular interest for this problem as all of the results presented here are for points sufficiently far away from the lower boundary so that the radiance values are independent of the surface albedo.

The downward normalized diffuse radiance is shown in Fig. 1 when $\omega_o = 0.99$ and $\omega_o = 0.9$ as a function of the cosine μ of the zenith angle of observation. These curves are in the principal plane, so that the azimuthal angle $\phi = 0°$ or $180°$. The cosine μ_o of the solar zenith angle is 0.85332 which corresponds to a zenith angle $\theta = 31.42°$. The downward radiance is shown for a number of different values of the optical depth τ within the medium. In each case the radiance is multiplied by the factor (π/diffuse flux at depth τ), so that variation of the radiance with μ at different depths can conveniently be compared. The incoming flux is normalized to unity across a plane at right angles to the incoming beam.

When $\omega_o = 0.99$, the downward radiance is a maximum at the horizon and has a minimum value just beyond the zenith on the antisolar side when $\tau < 1$. When $\tau = 8.9795$, the radiance has reached its asymptotic form predicted by Preisendorfer[8]. The curves for higher values of τ are not plotted, since they are identical with this last curve to the accuracy that can be shown in the figure. The asympotic radiance is, of course, symmetric around the zenith with a maximum value at the zenith.

The downward normalized interior radiance for $\omega_o = 0.9$, 0.5, and 0.1 is shown in Figs. 1, 2, and 3 respectively. The angular dependence of the radiance when $\tau \ll 1$ changes very little as ω_o decreases. On the other hand the angular dependence for large values of τ depends critically

on ω_o. The ratio of the radiance at the zenith to that at the horizon increases greatly as ω_o becomes smaller. The asymptotic form for the downward radiance is valid approximately when $\tau > 9$ provided that $\omega_o \geq 0.9$. On the other hand when $\omega_o \leq 0.5$ the asymptotic form has not developed even at $\tau = 40$. Although the existence of an asymptotic form has been predicted by Preisendorfer[8], the optical depth required for this angular distribution has not been known previously.

The variation of the flux and radiance as a function of optical depth is given for each case in Tables 1 - 6. Most of the quantities in these tables are discussed in a later section. The optical depth is given in the first column. In each case the lower boundary of the medium was taken at the largest optical depth shown in each table. A lower boundary surface of zero albedo was assumed. The seventh column of Tables 1 and 6 and the eighth column of Tables 2 - 5 give the ratio of the downward diffuse radiance at the zenith ($\mu = 1$) to that near the horizon ($\mu = 0.037850$ or $\theta = 87.83°$) when $\phi = 0°$ and $\mu_o = 0.85332$ (31.42°). When $\omega_o = 1$ (Table 1), this ratio is small near the upper boundary, becomes very slightly larger than unity in the interior of the medium, and then further increases to 2.71 at the lower boundary. When $\omega_o = 0.99$ (Table 2), the ratio has the limiting value of 1.20451 which is accurate to six significant figures when $16 < \tau < 69$. When $\omega_o = 0.9$ (Table 3), the asymptotic value is 2.13053 which is calculated to six significant figures when $32 < \tau < 65$; the ratio is within 10% of the asymptotic value when $8 < \tau < 73$.

However, the situation is quite different when $\omega_o = 0.5$ and 0.1 (Tables 4 and 5). The ratio continues to increase as τ increases in each of these cases and no asymptotic angular form develops when $\tau < 45$. Of

course, an asymptotic form would develop at sufficiently large values. However, it should be pointed out that the total downward flux is only 7.5×10^{-19} and 3.8×10^{-20} for $\omega_o = 0.5$ and 0.1 respectively at $\tau = 45$. The flux is normalized in these calculations to unit incoming solar flux per unit area perpendicular to the incoming beam. Thus when $\omega_o \leq 0.5$, the asymptotic angular form has not developed at optical depths such that the downward flux has been reduced to 10^{-20} of its original value. Experimental observation of the asymptotic form is out of the question under these conditions.

All of the values presented in Tables 1 - 5 assume that the sun is at the zenith. Selected values for other solar zenith angles are given in Table 6. The ratio of the downward flux already discussed is the same to six significant figures in the asymptotic region for $\mu_o = 0.18816$ ($\theta = 79.15°$) as for $\mu_o = 1.0$, when $\omega_o = 1, 0.99, 0.9$. On the other hand when $\omega_o = 0.5$, the ratio depends significantly on the solar zenith angle out to optical depths of the order of 50, as is shown in Fig. 4.

Even when $\tau = 50$ the ratio has a value that is an order of magnitude smaller when $\mu_o = 0.18816$ than when $\mu_o = 1$ for the case $\omega_o = 0.1$. From the slow convergence of these curves it would appear that an optical depth of the order of one thousand would be required before these curves would approach a limit and the asymptotic region would be reached. The flux would be of the order of 10^{-435} at such large optical depths and completely unobservable.

The prediction of Preisendorfer[8] that the asymptotic angular distribution becomes highly peaked in the forward direction as the single scattering albedo decreases is confirmed. However, our calculations show that the depth at which the asymptotic distribution develops also increases

as the single scattering albedo decreases. Even for the case $\omega_o = 0.9$, the downward flux is 4.5×10^{-8} of its original value at the beginning of the asymptotic region. Radiance values of this order cannot be detected experimentally against the background of other radiation sources. Thus, there is some limiting value of ω_o such that it becomes exceedingly difficult to observe the asymptotic radiance distribution for smaller values of ω_o. From the calculations given here it might be presumed that the limiting value is approximately $\omega_o = 0.8$.

All of the radiance values presented so far have been in the principal plane which contains the incident solar direction. Some examples of the azimuthal variation of the downward radiance are given in Figs. 5 and 6. As before the radiance has been multiplied in each case by the factor (π/diffuse flux at depth τ), so that the variation of the radiance with μ at different depths can conveniently be compared. The values $\mu_o = 0.85332$ (31.42°) and $\mu = 0.71392$ (44.44°) were chosen, since a fairly large azimuthal variation occurs for these values. When $\omega_o = 0.5$ the downward normalized interior radiance decreases as ϕ increases when τ is small. It reaches a maximum value when τ is about 3, and exhibits less and less dependence on ϕ as τ increases further. When $\tau = 32$, no variation with azimuth can be seen on the scale of the figure. The variation is qualitatively similar when $\omega_o = 0.1$, except that the variations are more pronounced. The curve is still decreasing when $\tau = 41$, since the asymptotic region has not yet been reached.

UPWARD RADIANCE

The upward normalized interior radiance is shown in Figs. 7, 8, and 9

when ω_o = 0.99, 0.5, and 0.1 respectively. The angular variation of the upward radiance is very much less than that of the downward and has been plotted on a linear scale. The radiance is these figures is shown as a function of the cosine μ of the nadir angle and is for the incident plane (ϕ = 0° or 180°). The solar horizon is on the left of all the figures. The cosine of the solar zenith angle was chosen as μ_o = 0.85332 (31.42°). In all cases the upward radiance has been normalized by multiplacation by the factor (π/diffuse flux at depth τ), as was previously explained.

When ω_o = 0.99 and the total optical depth of the medium is 109, the upward radiance near the upper surface of the medium has a minimum at the solar horizon, increases through the nadir, reaches a maximum value near a nadir angle of 50°, and then decreases toward the antisolar horizon. The upward normalized radiance increases at the horizon and decreases toward the nadir at greater optical depths within the medium. A limiting angular dependence of the normalized radiance is reached at about τ = 9 with a minimum at the nadir and a maxima at both the solar and antisolar horizons.

When ω_o = 0.5, Fig. 8 shows that the normalized upward radiance has a somewhat different form at small optical depths. It decreases from the solar horizon to a minimum value at a nadir angle of about 40° and then decreases uniformly through the nadir to the antisolar horizon. As the optical depth increases, the normalized upward radiance undergoes only a small change in its angular variation into its limiting angular dependence which must be symmetric around the nadir. This limiting form occurs at about τ = 25.

The normalized upward radiance when ω_o = 0.1 is shown in Fig. 9. The angular variation at small optical depths has the same qualitative

variation as was shown for the previous case. The asymptotic angular variation has not been reached even at $\tau = 42$, although the curve is beginning to show only a small variation with τ. In this case the asymptotic curve appears to have a minimum near a nadir angle of 55° and a relative maximum at the nadir and the horizon.

The variation of the normalized upward radiance with azimuthal angle is relatively small as is shown in Fig. 10. The following parameters were selected for this illustration: $\mu_o = 0.85332$ (31.42°), $\mu = 0.71392$ (44.44°), and $\omega_o = 0.5$. At small optical depths within the medium the radiance increases slowly as ϕ increases from 0° and 180°. There is no appreciable azimuthal variation when $\tau > 17$.

The sixth column of Tables 1 and 6 and the seventh column of Tables 2 - 5 give the ratio of the upward radiance at the nadir ($\mu = 1$) to that near the horizon ($\mu = 0.03785$ or $\theta = 87.83°$). The limiting value for this ratio holds over approximately the same range of optical depths as for the corresponding ratio for the downward radiance already discussed. The limiting value for the ratio for the upward radiance in the interior of the medium is 0.99994, 0.86137, and 0.69386 when $\omega_o = 1.0$, 0.99, and 0.9 respectively. The ratio for the upward radiance does not vary over as wide a range as that for the downward radiance. For example, when $\omega_o = 0.1$, the ratio for the upward radiances is 1.0300 at the upper boundary and has changed only to 0.9422 at an optical depth of 40.98, while the corresponding ratio for the downward radiance varies from 0.075 to 75.6.

FLUX

Flux values at various optical depths within the medium as given in Table 1 when $\omega_o = 1$. The second column gives the upward flux; the third

column shows the downward diffuse flux; the fourth column gives the total downward flux including the incident solar beam which is assumed to be at the zenith. The difference between the total downward flux and the upward flux is shown in the fifth column. The upward and downward flux have the same numerical value to four or five significant figures. Nevertheless their difference is constant to four significant figures in our calculations. The difference is necessarily a constant for a conservative problem ($\omega_o = 1$). The incident solar beam makes no contribution to the total downward flux to five significant figures at optical depths greater than 13. The total downward flux becomes significantly greater than unity over a large range of optical depths starting from the upper surface, a phenomenon which does not violate the conservation of energy. The explanation is similar to that given by Plass and Kattawar[9] for the fact that the downward flux from the lower surface of a medium may be greater than unity under certain conditions.

The first four columns in Tables 2 - 5 tabulate the same quantitites as are in Table 1. The fifth column of Tables 2 - 5 shows the ratio of the upward flux to the total downward flux. The quantity $\partial F/\partial\tau$, which is proportional to the heating rate of the layer, is given in the sixth column. Within the tabulated accuracy of four significant figures, the incident beam does not contribute to the total flux at optical depths greater than 17 when $\omega_o = 0.99$ or 0.9. However, the situation is quite different when $\omega_o = 0.5$. The total downward flux is 7.5×10^{-9} at $\tau = 45$ and yet the direct beam is still contributing 4% of the total flux value. Similarly when $\omega_o = 0.1$, the total downward flux is 3.4×10^{-20} at $\tau = 45$, so that the direct beam is contributing 77% of the total downward flux. Since the

contribution of the direct beam to the total downward flux is 2.9×10^{-20} at this optical depth, this is a lower limit for the total downward flux no matter how small ω_o may be. When $\omega_o \leq 0.5$ and $\mu_o = 1$, a significant number of the photons occurring at great depths have been a part of the unscattered direct beam until these depths are reached.

The ratio of the upward interior flux to the total downward interior flux is often measured experimentally. When $\omega_o = 0.99$, this ratio is remarkably constant except near the lower boundary. The tabulated values range only from 0.753 to 0.793. The ratio has the constant value 0.793 when $9 \leq \tau \leq 85$. Similarly the ratio has the constant value 0.470 when $17 \leq \tau \leq 65$ and $\omega_o = 0.9$. This ratio only varies over a range of 2%, 5%, 5%, and 1% from an optical depth of unity to near the lower boundary of the medium for $\omega_o = 0.99, 0.9, 0.5, 0.1$ respectively. The physical explanation for the constancy of this ratio is that the upward flux is derived by multiple scattering from the downward flux, so that the ratio varies with optical depth within the medium only as other factors change the relative contributions of the scattering above and below the point that is being considered. Thus the ratio would be expected to be constant in the region where the asymptotic radiance distribution holds as well as approximately constant at all optical depths except those very close to boundaries.

The quantity $\partial F/\partial\tau$, which is proportional to the heating rate, is also given in Tables 2 - 5. In all cases it is proportional to the total downward flux when $\tau > 1$ and the interior point is not too near the lower boundary. In all cases the heating rate increases as the optical depth increases starting from the upper boundary and reaches a maximum when τ is approximately 1, 0.25, and 0.01 when $\omega_o = 0.99, 0.9$, and 0.5 respectively.

Since all of the data in Tables 1 - 5 are for the case $\omega_o = 1$, some selected data for other values of μ_o are shown in Table 6. The ratio of the upward to the total downward flux is given in column five. This ratio in the asymptotic region is 0.793 and 0.470 for $\omega_o = 0.99$ and 0.9 respectively when $\mu_o = 0.18816$ ($\theta_o = 79.15°$). This agrees exactly with the asymptotic value given in Tables 2 and 3 for $\mu_o = 1$. When $\omega_o = 0.5$ the asymptotic value for this ratio differs only in the fourth significant figure for different values of μ_o (Tables 4 and 6). When $\omega_o = 0.1$, this ratio had not approached its limiting value even at $\tau = 41$. The value of the ratio at $\tau = 41$ is 0.01805, 0.01826, and 0.01820 for $\mu_o = 1$, 0.8332, and 0.18816 when $\omega_o = 0.1$. In the true asymptotic region the value of this ratio should be independent of μ_o.

The ratio of the direct downward flux to the total downward flux is given in the fourth column of Table 6. It is important to understand the range of optical depths over which the direct flux is an important part of the total flux. For example, when $\omega_o = 0.1$ and $\mu_o = 1$, Table 5 shows that the direct flux is more than 10% of the total for all $\tau < 45$. From Table 6 and additional data from the original calculation we find that the direct flux is more than 10% of the total when $\tau < 33$ for $\mu_o = 0.85332$ (31.42°) and when $\tau < 1.5$ for $\mu_o = 0.18816$ (79.15°). Thus in this case when the single scattering albedo is small the importance of the direct beam depends critically on the solar zenith angle. The exponential degradation of the solar beam measured along the vertical is, of course, much more rapid when the sun is near the horizon increasing as sec θ. It is also interesting to study how rapidly this ratio decreases with optical depth for other values of ω_o from Table 6.

The total downward flux decreases exponentially when the optical depth is sufficiently great and the point of observation is not too close to the lower boundary. The decrease with optical depth of the total downward flux can be represented quite accurately with exp $(-b\tau)$, where $b = 0.17244$ and 0.52318 for $\omega_o = 0.99$ and 0.9 respectively, provided that $\tau > 3$ and is not near the lower boundary. However, when the absorption is relatively large ($\omega_o \leq 0.5$), only an approximate fit can be obtained with $b = 0.944$ when $\omega_o = 0.5$ and $b = 0.997$ when $\omega_o = 0.1$. The reason for the approximate fit is two-fold: (1) the direct beam is a significant fraction of the total downward flux even up to $\tau = 40$ for normal incidence with large absorption. Since the direct beam decays at a different rate than the diffuse flux, the latter rate cannot be established until the direct beam is no longer contributing a majority of the photons in the vicinity. (2) When the absorption is large, a majority of the photons at great optical depths arise from single scattering events at smaller optical depths which scatter the photon out of the direct beam into a nearly vertical direction. The number of photons which have undergone single scattering and reached large optical depths decreases with optical depth as $\exp(-\tau)$. Deviations from this rate of decrease for the total flux are due to photons that have undergone higher orders of scattering. An equilibrium between the number of photons that have undergone various orders of scattering is not obtained in the case of large absorption until very large optical depths are reached.

The development of the exponential decrease in both the flux and radiance is shown in Fig. 11 for the case when $\omega_o = 0.1$. The radiance or flux is shown as a function of the optical depth within the medium. In each case the dashed line represents a pure exponential dependence obtained by fitting

the curve at large optical depths. On the rather small scale of this figure deviations are observed up to optical depths of the order of 20. The actual calculations show that there are still deviations from the pure exponential as large as 1% at $\tau = 40$.

The upper curve in Fig. 11 shows the flux for $\mu_o = 1$, while the next curve gives the flux for $\mu_o = 0.18816$ (79.15°). In the first case the actual flux for $\tau < 20$ is below, while in the second case it is above, the value given by the pure exponential indicated by dashed lines in the figure. The downward radiance is shown for five different values of μ (1, 0.92226; 0.81141; 0.47254; 0.037850) when $\mu_o = 0.18816$. The downward radiance near the zenith is much larger than that nearer the horizon for large τ due to the large maximum that develops at the zenith (see Fig. 3). The downward radiance near the zenith approaches the limiting exponential curve from below as τ increases, while it approaches it from above for larger zenith angles. For this particular case, the downward radiance at the zenith ($\mu = 1$) decreases exponentially with the optical depth within the accuracy of Fig. 11 when $\tau > 2$, while the downward radiance for $\mu = 0.47154$ decreases exponentially only when $\tau > 20$. Thus the pure exponential decrease develops at much smaller values of the optical depth for the radiance near the zenith than near the horizon.

CONCLUSIONS

The interior radiance and flux have been studied for a very thick Rayleigh scattering absorbing layer. Their dependence on the solar zenith angle, the single scattering albedo, and the optical depth within the medium has been shown. The development of an asymptotic angular form for the downward radiance as predicted by Preisendorfer is confirmed. A range of optical

depths is given for each case for which this asymptotic form is valid. When $\omega_o < 0.8$, the asymptotic form only develops at great optical depths such that the downward flux is 10^{-8} or less of its value at the upper boundary. Thus in this case the flux is so small that the asymptotic form could not be observed experimentally. As an example, when $\omega_o = 0.1$, the asymptotic form has not developed even at $\tau = 41$, at which depth the downward flux is 2×10^{-18} times its value at the upper boundary.

The ratio of the upward to the downward flux is remarkably constant within the medium. This ratio never varies by more than 5% from an optical depth of unity to near the lower boundary of the medium for any value of the single scattering albedo. Over the same range of optical depths within the medium, the heating rate is found to be proportional to the total downward flux.

When $\omega_o \geq 0.9$ the total downward flux decreases exponentially with optical depth provided $\tau > 3$ and is not near the lower boundary. However when $\omega_o \leq 0.5$, only an approximate exponential fit can be obtained at least down to optical depths of 40 where the flux is so small as to be experimentally unobservable. When $\omega_o \leq 0.5$, the direct flux makes an important contribution to the total flux down to optical depths of the order of 45. For example, when $\omega_o = 0.1$ and $\mu_o = 1$, the direct flux is more than 10% of the total flux for all $\tau < 45$.

This work was supported in part by Grant No. NGR 44-001-117 from the National Aeronautics and Space Administration. Acknowledgment is made to the National Center for Atmospheric Research, which is sponsored by the National Science Foundation, for computer time used in this research.

REFERENCES

1. G. N. Plass, G. W. Kattawar, and F. E. Catchings, Appl. Opt., (accepted for publication).
2. G. W. Kattawar and G. N. Plass, J. Quant. Spect. and Rad. Trans. (submitted as Part I of this paper).
3. G. N. Plass and G. W. Kattawar, Appl. Opt. 8, 455 (1969).
4. G. N. Plass and G. W. Kattawar, J. Phys. Oceanography 2, 139 (1972).
5. G. W. Kattawar and G. N. Plass, J. Phys. Oceanography 2, 146 (1972).
6. R. Bellman, Introduction to Matrix Analysis, McGraw Hill Book Co., New York (1960).
7. G. W. Kattawar, J. Quant. Spect. and Rad. Trans. (accepted for publication).
8. R. W. Preisendorfer, J. Marine Res. 18, 1 (1959).
9. G. N. Plass and G. W. Kattawar, Appl. Opt. 7, 699 (1968).

TABLE 1

$\omega_o = 1, \quad \mu_o = 1$

Optical Depth	F^{up}	$F^{down}_{diffuse}$	F^{down}_{total}	$F^{down}_{total} - F^{up}$	$I^{up}(1)/I^{up}(0.03785)$	$I^{down}(1)/I^{down}(0.03785)$
0	0.9999	0	1.0000	1.004 -4	1.57779	
0.125	1.0443	0.1619	1.0444	1.004 -4	1.38629	0.14608
0.25	1.0781	0.2994	1.0782	1.004 -4	1.29104	0.24696
0.5	1.1282	0.5217	1.1283	1.004 -4	1.18434	0.40630
1	1.1888	0.8211	1.1889	1.004 -4	1.08845	0.61795
5	1.2635	1.2569	1.2636	1.004 -4	1.00096	0.98839
13	1.2639	1.2640	1.2640	1.004 -4	0.99994	1.00005
77	1.2591	1.2592	1.2592	1.004 -4	0.99994	1.00006
205	1.2495	1.2496	1.2496	1.004 -4	0.99994	1.00006
8,397	0.6324	0.6325	0.6325	1.004 -4	0.99988	1.00011
16,589	1.544 -2	1.544 -2	1.544 -2	1.004 -4	0.99532	1.00468
16,717	5.802 -3	5.903 -3	5.903 -3	1.004 -4	0.98761	1.01238
16,781	9.824 -4	1.083 -3	1.083 -3	1.004 -4	0.92963	1.06998
16,793	7.820 -5	1.786 -4	1.786 -4	1.004 -4	0.48306	1.56051
16,793.875	1.038 -5	1.107 -4	1.107 -4	1.004 -4	0.12149	2.29156
16,794	0	1.004 -4	1.004 -4	1.004 -4		2.71294

TABLE 2

$\omega_o = 0.99, \quad \mu_o = 1$

Optical Depth	F^{up}	$F^{down}_{diffuse}$	F^{down}_{total}	F^{up}/F^{down}_{total}	$\frac{\partial F}{\partial \tau}$	$I^{up}(1)/I^{up}(0.03765)$	$I^{down}(1)/I^{down}(0.03785)$
0	0.7527	0	1.0000	0.753		1.39298	
0.000977	0.7529	1.174 -3	1.0002	0.753	2.436 -2	1.39077	0.05219
0.00293	0.7534	3.515 -3	1.0006	0.753	2.446 -2	1.38644	0.05341
0.01074	0.7550	1.278 -2	1.0021	0.753	2.480 -2	1.37015	0.05848
0.04199	0.7611	4.844 -2	1.0073	0.756	2.592 -2	1.31739	0.08104
0.1045	0.7705	0.1143	1.0150	0.759	2.746 -2	1.24483	0.13350
0.4795	0.7917	0.4059	1.0250	0.772	3.161 -2	1.05250	0.41733
0.9795	0.7756	0.6172	0.9927	0.781	3.276 -2	0.95979	0.65973
2.98	0.5950	0.7009	0.7517	0.792	2.652 -2	0.87438	1.07010
8.98	0.2145	0.2703	0.2704	0.793	9.639 -3	0.86144	1.20293
16.98	5.399 -2	6.807 -2	6.807 -2	0.793	2.426 -3	0.86137	1.20451
24.98	1.359 -2	1.713 -2	1.713 -2	0.793	6.108 -4	0.86137	1.20451
32.98	3.421 -3	4.312 -3	4.312 -3	0.793	1.537 -4	0.86137	1.20451
40.98	8.611 -4	1.086 -3	1.086 -3	0.793	3.870 -5	0.86137	1.20451
52.98	1.087 -4	1.371 -4	1.371 -4	0.793	4.887 -6	0.86137	1.20451
68.98	6.890 -6	8.685 -6	8.685 -6	0.793	3.096 -7	0.86137	1.20451
84.98	4.364 -7	5.502 -7	5.502 -7	0.793	1.961 -8	0.86130	1.20457
92.98	1.094 -7	1.382 -7	1.382 -7	0.792	4.922 -9	0.86028	1.20557
.00.98	2.593 -8	3.350 -8	3.350 -8	0.774	1.181 -9	0.84328	1.22211
.08.98	0	3.235 -9	3.235 -9	0.000	5.560 -11		2.79757

TABLE 3

$\omega_o = 0.9, \mu_o = 1$

Optical Depth	F^{up}	$F^{down}_{diffuse}$	F^{down}_{total}	F^{up}/F^{down}_{total}	$\frac{\partial F}{\partial \tau}$	$I^{up}(1)/I^{up}(0.03785)$	$I^{down}(1)/I^{down}(0.03785)$
0	0.4183	0	1.0000	0.418		1.16154	
0.000977	0.4183	7.984 -4	0.9998	0.418	0.1822	1.15990	0.05681
0.00293	0.4183	2.389 -3	0.9995	0.418	0.1826	1.15666	0.05815
0.01074	0.4182	8.669 -3	0.9980	0.419	0.1844	1.14448	0.06368
0.04199	0.4176	3.262 -2	0.9915	0.421	0.1898	1.10484	0.08844
0.1045	0.4148	7.587 -2	0.9766	0.425	0.1957	1.04972	0.14684
0.2295	0.4058	0.1479	0.9428	0.430	0.2002	0.97896	0.27068
0.4795	0.3806	0.2486	0.8677	0.439	0.1975	0.89709	0.48340
0.9795	0.3204	0.3384	0.7139	0.449	0.1749	0.81625	0.80526
2.98	0.1304	0.2303	0.2811	0.464	7.553 -2	0.72391	1.52815
8.98	6.007 -3	1.267 -2	1.280 -2	0.469	3.546 -3	0.69507	2.07690
16.98	9.164 -5	1.951 -4	1.951 -3	0.470	5.414 -5	0.69388	2.12884
24.98	1.394 -6	2.968 -6	2.968 -6	0.470	8.237 -7	0.69386	2.13048
32.98	2.121 -8	4.516 -8	4.516 -8	0.470	1.253 -8	0.69386	2.13053
40.98	3.227 -10	6.870 -10	6.870 -10	0.470	1.906 -10	0.69386	2.13053
48.98	4.909 -12	1.045 -11	1.045 -11	0.470	2.900 -12	0.69386	2.13053
56.98	7.468 -14	1.590 -13	1.590 -13	0.470	4.412 -14	0.69386	2.13053
64.98	1.136 -15	2.419 -15	2.419 -15	0.470	6.712 -16	0.69385	2.13053
72.98	1.704 -17	3.668 -17	3.668 -17	0.464	1.014 -17	0.68433	2.13978
76.98	0	3.508 -18	3.508 -18	0.000	5.787 -19		3.76160

TABLE 4

$\omega_o = 0.5, \quad \mu_o = 1$

Optical Depth	F^{up}	$F^{down}_{diffuse}$	F^{down}_{total}	F^{up}/F^{down}_{total}	$\frac{\partial F}{\partial \tau}$	$I^{up}(1)/I^{up}(0.03785)$	$I^{down}(1)/I^{down}(0.03785)$
0	0.1207	0	1.0000	0.1207		1.02562	
0.000977	0.1206	3.023 -4	0.9993	0.1207	0.6204	1.02483	0.06727
0.00293	0.1205	9.036 -4	0.9980	0.1207	0.6204	1.02328	0.06890
0.01074	0.1199	3.265 -3	0.9926	0.1208	0.6205	1.01742	0.07563
0.04199	0.1177	1.209 -2	0.9710	0.1212	0.6176	0.99812	0.10620
0.1045	0.1130	2.736 -2	0.9282	0.1217	0.6038	0.97058	0.18106
0.4795	8.652 -2	7.814 -2	0.6972	0.1241	0.4834	0.88725	0.68001
0.9795	5.863 -2	9.047 -2	0.4660	0.1258	0.3361	0.83598	1.26512
2.98	1.084 -2	3.331 -2	8.412 -2	0.1289	6.445 -2	0.76045	3.19766
8.98	4.842 -5	2.433 -4	3.692 -4	0.1311	2.953 -4	0.70911	7.58946
16.98	2.886 -8	1.764 -7	2.187 -7	0.1320	1.775 -7	0.69198	11.8779
24.98	1.592 -11	1.061 -10	1.203 -10	0.1323	9.819 -11	0.68540	15.0246
32.98	8.487 -15	5.930 -14	6.406 -14	0.1325	5.243 -14	0.68219	17.3462
40.98	4.445 -18	3.194 -17	3.354 -17	0.1325	2.749 -17	0.67994	19.0513
44.98	0	7.200 -19	7.492 -19	0.0000	5.003 -19		24.3430

TABLE 5

$\omega_o = 0.1 \quad \mu_o = 1$

ptical Depth	F^{up}	$F^{down}_{diffuse}$	F^{down}_{total}	F^{up}/F^{down}_{total}	$\frac{\partial F}{\partial \tau}$	$I^{up}(1)/I^{up}(0.03785)$	$I^{down}(1)/I^{down}(0.03783)$
0	1.777 -2	0	1.0000	1.777 -2		1.0300	
0.000977	1.775 -2	5.044 -5	0.9991	1.777 -2	0.9310	1.0298	0.07483
0.00293	1.772 -2	1.506 -4	0.9972	1.777 -2	0.9296	1.0295	0.07668
0.01704	1.760 -2	5.428 -4	0.9898	1.778 -2	0.9236	1.0283	0.08439
0.04199	1.709 -2	1.989 -3	0.9609	1.778 -2	0.8994	1.0245	0.1198
0.1045	1.611 -2	4.423 -3	0.9052	1.780 -2	0.8507	1.0189	0.2092
0.4795	1.126 -2	1.175 -2	0.6308	1.785 -2	0.5995	1.0008	0.8714
0.9795	6.948 -3	1.266 -2	0.3882	1.790 -2	0.3714	0.9886	1.750
2.98	9.810 -4	3.785 -3	5.460 -2	1.797 -2	5.281 -2	0.9687	5.158
8.98	2.593 -6	1.797 -5	1.439 -4	1.802 -2	1.403 -4	0.9532	15.069
6.98	9.117 -10	8.289 -9	5.005 -8	1.804 -2	4.941 -8	0.9474	28.054
4.98	3.156 -13	3.314 -12	1.749 -11	1.804 -2	1.712 -11	0.9449	40.929
2.98	1.084 -16	1.253 -15	6.008 -15	1.804 -2	5.884 -15	0.9435	53.740
0.98	3.709 -20	4.596 -19	2.055 -18	1.805 -2	2.013 -18	0.9422	66.505
4.98	0	8.724 -21	3.794 -20	0	3.592 -20		75.629

Optical Depth	ω_o	μ_o	$\frac{F^{down}_{direct}}{F^{down}_{total}}$	F^{up}/F^{down}_{total}	$I^{up}(1)/I^{up}(0.03785)$	$I^{down}(1)/I^{down}(0.03785)$
8,397	1	0.18816		0.9998	0.99988	1.00011
16.98	0.99	0.18816	2.038 -38	0.793	0.86137	1.20451
68.98	0.99	0.18816	1.529 -154	0.793	0.86137	1.20451
32.98	0.9	0.18816	4.859 -69	0.470	0.69386	2.13053
56.98	0.9	0.18816	3.083 -132	0.470	0.69386	2.13053
24.98	0.5	0.85332	5.492 -3	0.1329	0.67380	19.257
32.98	0.5	0.85332	9.277 -4	0.1328	0.67633	20.981
40.98	0.5	0.85332	1.550 -4	0.1327	0.67670	21.928
24.98	0.5	0.18816	3.677 -47	0.1328	0.67602	20.381
32.98	0.5	0.18816	2.492 -62	0.1328	0.67702	21.560
40.98	0.5	0.18816	1.681 -77	0.1327	0.67694	22.251
2.98	0.1	0.85332	0.9069	1.906 -2	0.65813	4.5792
8.98	0.1	0.85332	0.7680	1.902 -2	0.67232	23.200
24.98	0.1	0.85332	0.2990	1.860 -2	0.77947	225.66
40.98	0.1	0.85332	4.225 -2	1.826 -2	0.87746	600.35
0.9795	0.1	0.18816	0.3371	2.556 -2	0.21390	5.1162
2.98	0.1	0.18816	1.789 -4	1.956 -2	0.63417	59.434
8.98	0.1	0.18816	2.279 -15	1.864 -2	0.79219	176.27
16.98	0.1	0.18816	3.807 -30	1.838 -2	0.85190	323.16
24.98	0.1	0.18816	5.264 -45	1.828 -2	0.87704	463.12
32.98	0.1	0.18816	6.695 -60	1.823 -2	0.89087	598.26
40.98	0.1	0.18816	8.121 -75	1.820 -2	0.89931	729.76

FIGURE CAPTIONS

Fig. 1. Downward normalized interior radiance as a function of the cosine (μ) of the zenith angle. Curves are given for various values of the optical depth within a very thick homogenous layer scattering according to the Rayleigh phase function. The upper curves are for ω_o=0.99 and the lower curves for ω_o=0.9. In each case the radiance has been multiplied by the factor (π / diffuse flux at depth τ), so that the variation of the radiance with μ at different depths can conveniently be compared. These curves are for μ_o=0.85332 (31.42^o) and the incident plane containing the direction of the incoming beam (ϕ = 0^o for left half and ϕ = 180^o for right half of figure). The solar horizon is at the left of the figure, the zenith is at the center, and the antisolar horizon is at the right of the figure. The incoming flux is normalized to unity across a plane at right angles to the incoming beam.

Fig. 2. Downward normalized interior radiance for ω_o = 0.5 and μ_o = 0.85332. See caption to Fig. 1.

Fig. 3. Downward normalized interior radiance for ω_o=0.1 and μ_o=0.85332. See caption to Fig. 1.

Fig. 4. The ratio of the downward interior radiance at μ = 1 to the downward interior radiance at μ = 0.03785 (θ = 87.83^o) as a function of the optical depth within the medium. Curves are given for ω_o = 0.99, 0.9, 0.5, and 0.1 and for μ_o = 1, μ_o = 0.85332 (θ = 31.42^o), μ_o = 0.53786 (θ_o = 57.46^o), and μ_o = 0.18816 (θ_o = 79.15^o).

Fig. 5. Downward normalized interior radiance for ω_o = 0.5, μ_o = 0.85332 (θ_o = 31.42^o), and μ = 0.71392 (44.44^o) as a function of the azimuthal angle ϕ.

Fig. 6. Downward normalized interior radiance for $\omega_o = 0.1$, $\mu_o = 0.85332$ ($\theta_o = 31.42^o$), and $\mu = 0.71392$ (44.44^0) as a function of the azimuthal angle ϕ.

Fig. 7. Upward normalized interior radiance as a function of the cosine (μ) of the nadir angle. These curves are for $\mu_o = 0.85332$ (31.42^o) and the incident plane ($\phi = 0^o$ and 180^o). See caption to Fig. 1.

Fig. 8. Upward normalized interior radiance for $\mu_o = 0.85332$ and $\omega_o = 0.5$. See caption to Fig. 1.

Fig. 9. Upward normalized interior radiance for $\mu_o = 0.85332$ and $\omega_o = 0.1$. See caption to Fig. 1.

Fig. 10. Upward normalized interior radiance for $\omega_o = 0.5$, $\mu_o = 0.85332$ ($\theta = 31.42^o$), and $\mu = 0.71392$ (44.44^o) as a function of the azimuthal angle ϕ.

Fig. 11. The interior downward radiance or flux as a function of the optical depth within a very thick homogenous layer for $\omega_o = 0.1$. The upper curve is the downward flux for $\mu_o = 1$ and the next curve is for $\mu_o = 0.18816$ $(79.15)^o$. The next curves in order give the downward radiance for $\mu_o = 0.18816$ (79.15^o) and the following five values for μ : 1(0.00^o); 0.92226 (22.74^o); 0.81141 (35.77^o); 0.47254 (61.80^o); 0.03785 (87.83^o). The azimuthal angle $\phi = 0^o$. The dashed lines indicate an exponential fitted at large optical depths.

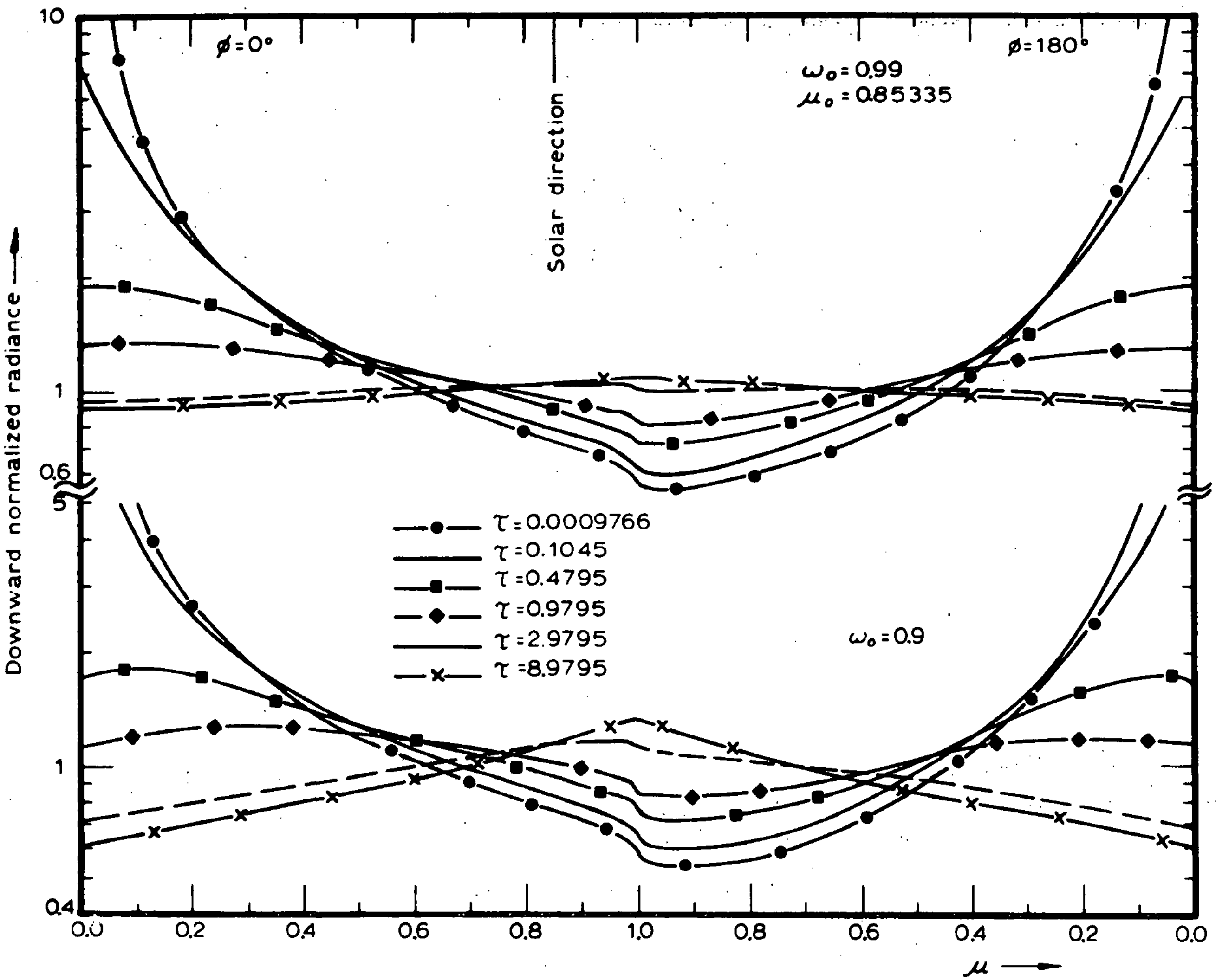

10
φ=0°
Solar direction
ω₀=0.99
μ₀=0.85335
φ=180°
1
0.6
5
τ=0.0009766
τ=0.1045
τ=0.4795
τ=0.9795
τ=2.9795
τ=8.9795
ω₀=0.9
Downward normalized radiance
0.4
0.0
0.2
0.4
0.6
0.8
1.0
0.8
0.6
0.4
0.2
0.0
μ

Fig. 1

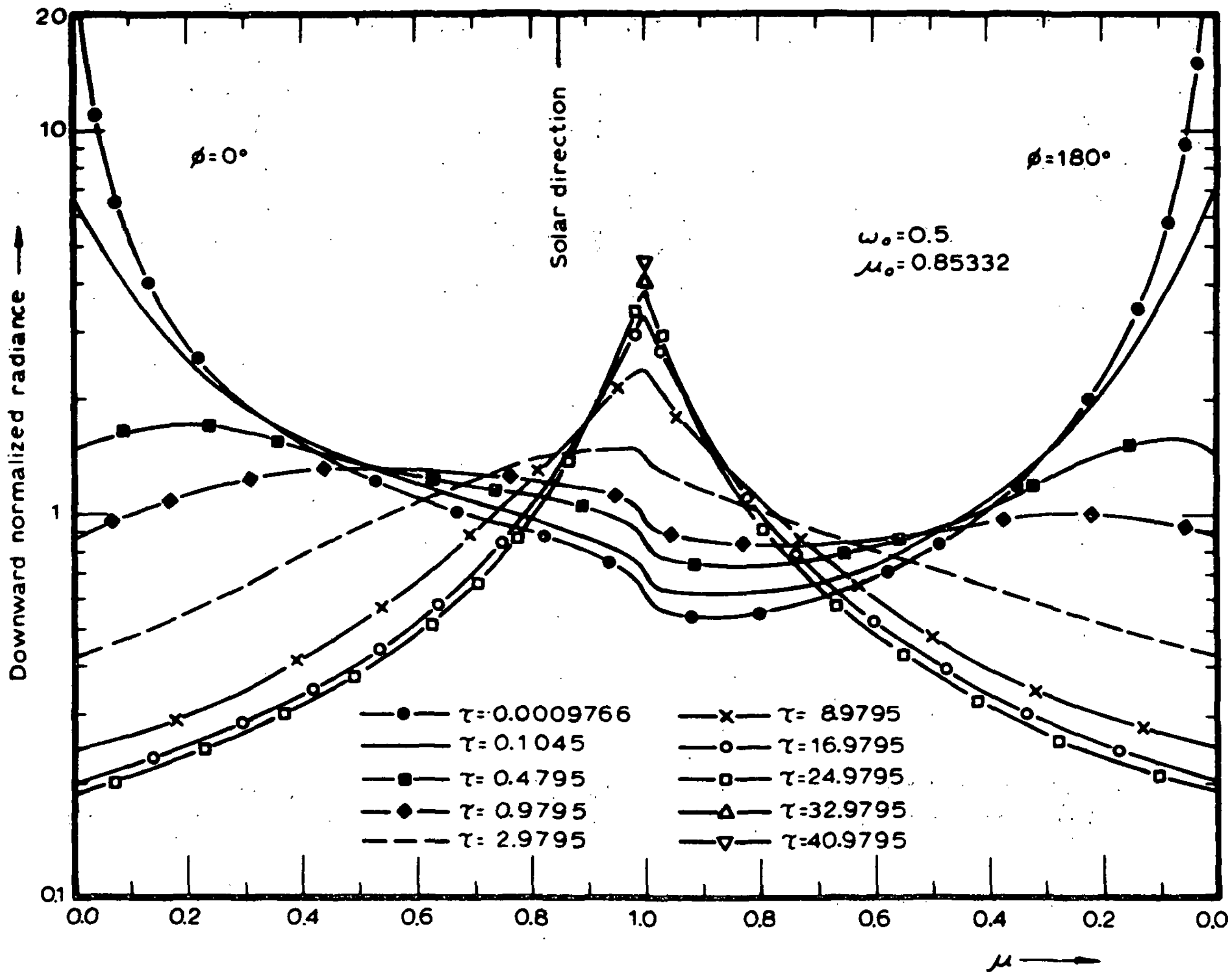

Solar direction
ϕ=0°
ϕ=180°
ω₀=0.5
μ₀=0.85332
Downward normalized radiance
μ
τ=0.0009766
τ=0.1045
τ=0.4795
τ=0.9795
τ=2.9795
τ=8.9795
τ=16.9795
τ=24.9795
τ=32.9795
τ=40.9795
20
10
1
0.1
0.0
0.2
0.4
0.6
0.8
1.0
0.8
0.6
0.4
0.2
0.0

Fig. 2

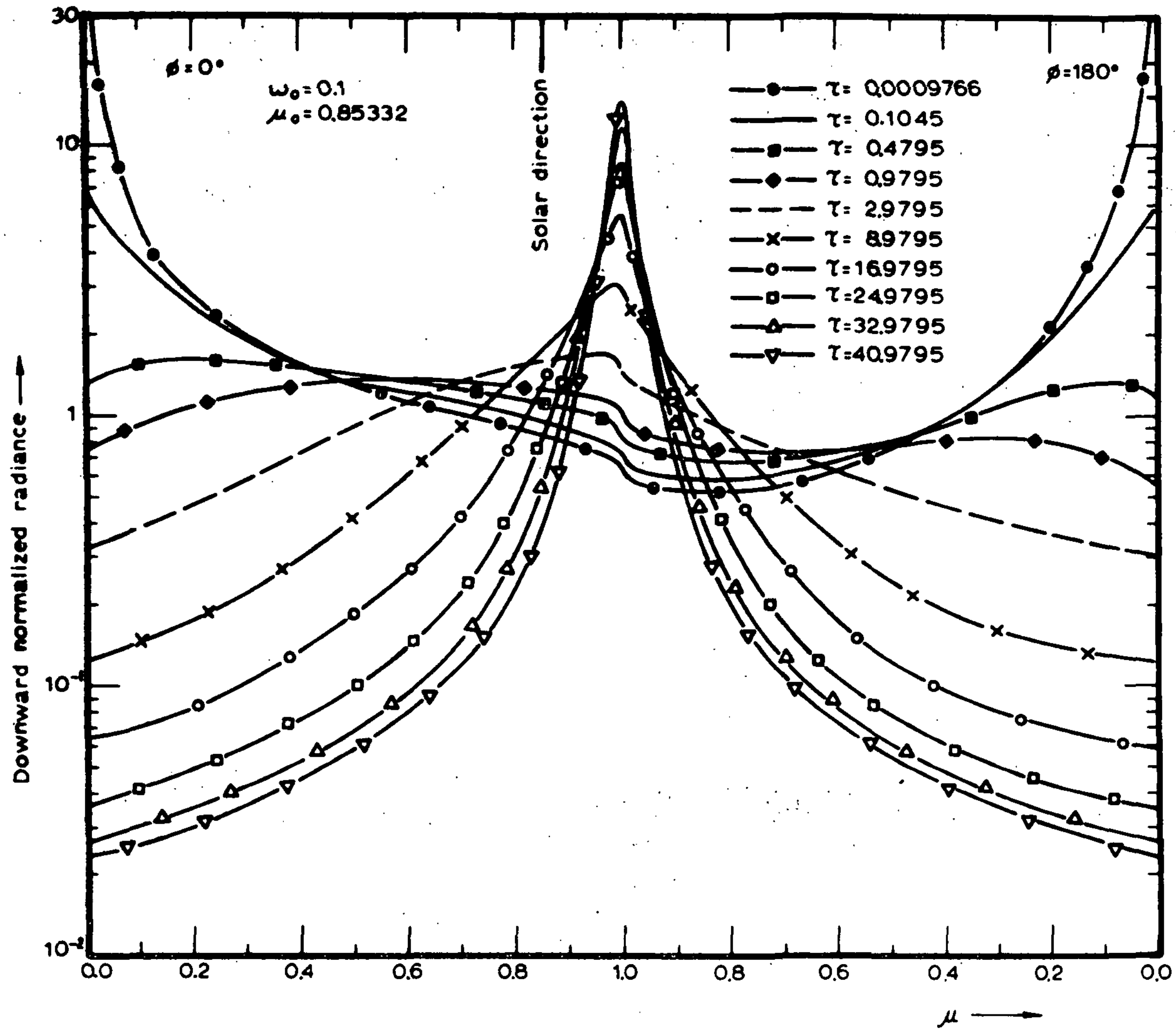

φ=0°
ω₀=0.1
μ₀=0.85332
Solar direction
τ= 0.0009766
τ= 0.1045
τ= 0.4795
τ= 0.9795
τ= 2.9795
τ= 8.9795
τ=16.9795
τ=24.9795
τ=32.9795
τ=40.9795
φ=180°
Downward normalized radiance
μ

Fig. 3

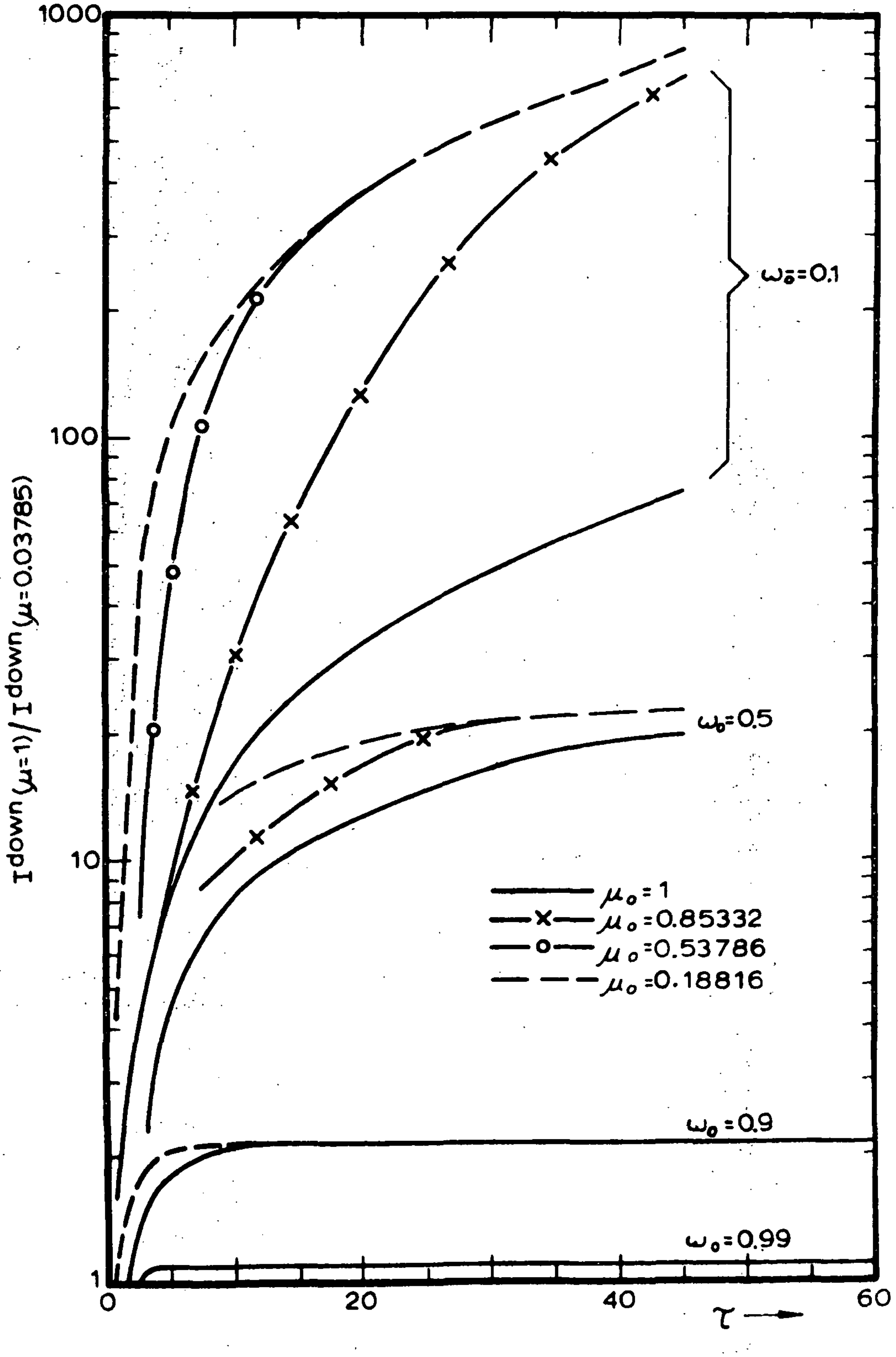
1000
100
10
1
0
20
40
60
τ
$I^{down}(\mu=1)/I^{down}(\mu=0.03785)$
$\omega_0=0.1$
$\omega_0=0.5$
$\omega_0=0.9$
$\omega_0=0.99$
$\mu_0=1$
$\mu_0=0.85332$
$\mu_0=0.53786$
$\mu_0=0.18816$

Fig. 4

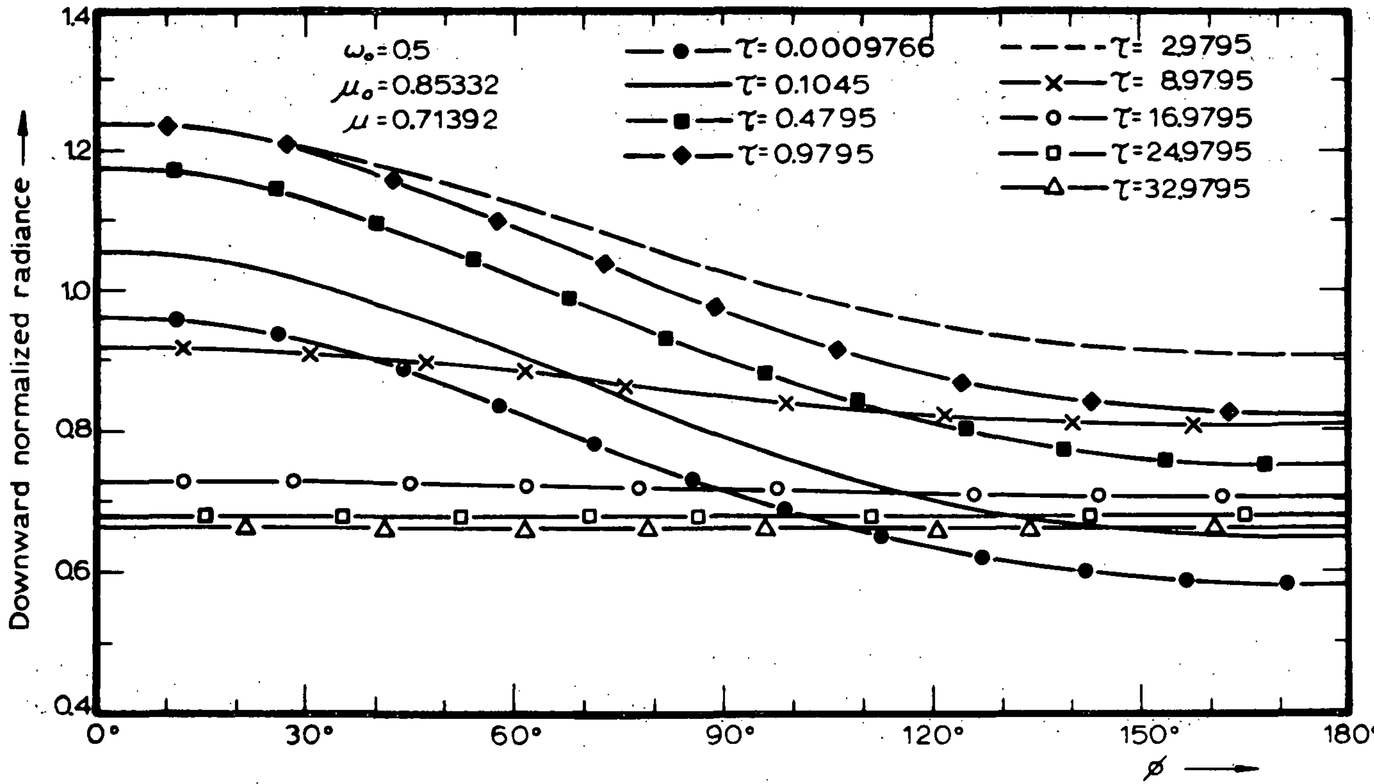

ω_o=0.5
μ_o=0.85332
μ=0.71392
τ= 0.0009766
τ= 0.1045
τ= 0.4795
τ= 0.9795
τ= 2.9795
τ= 8.9795
τ= 16.9795
τ= 24.9795
τ= 32.9795
Downward normalized radiance
1.4
1.2
1.0
0.8
0.6
0.4
0°
30°
60°
90°
120°
150°
180°
ϕ

Fig. 5

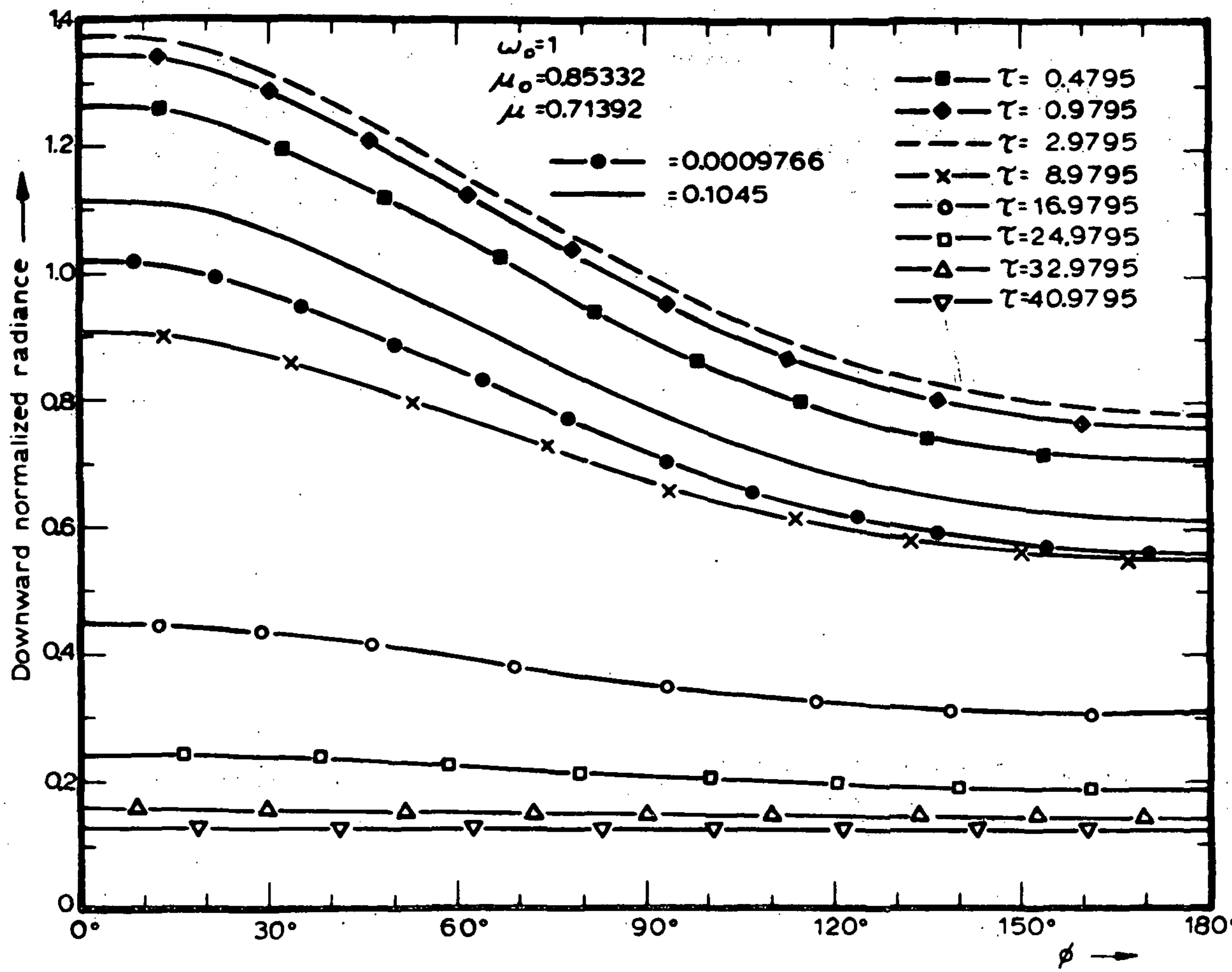

ω_o=1
μ_o=0.85332
μ =0.71392
=0.0009766
=0.1045
τ= 0.4795
τ= 0.9795
τ= 2.9795
τ= 8.9795
τ=16.9795
τ=24.9795
τ=32.9795
τ=40.9795
Downward normalized radiance
1.4
1.2
1.0
0.8
0.6
0.4
0.2
0
0°
30°
60°
90°
120°
150°
180°
ϕ

Fig. 6

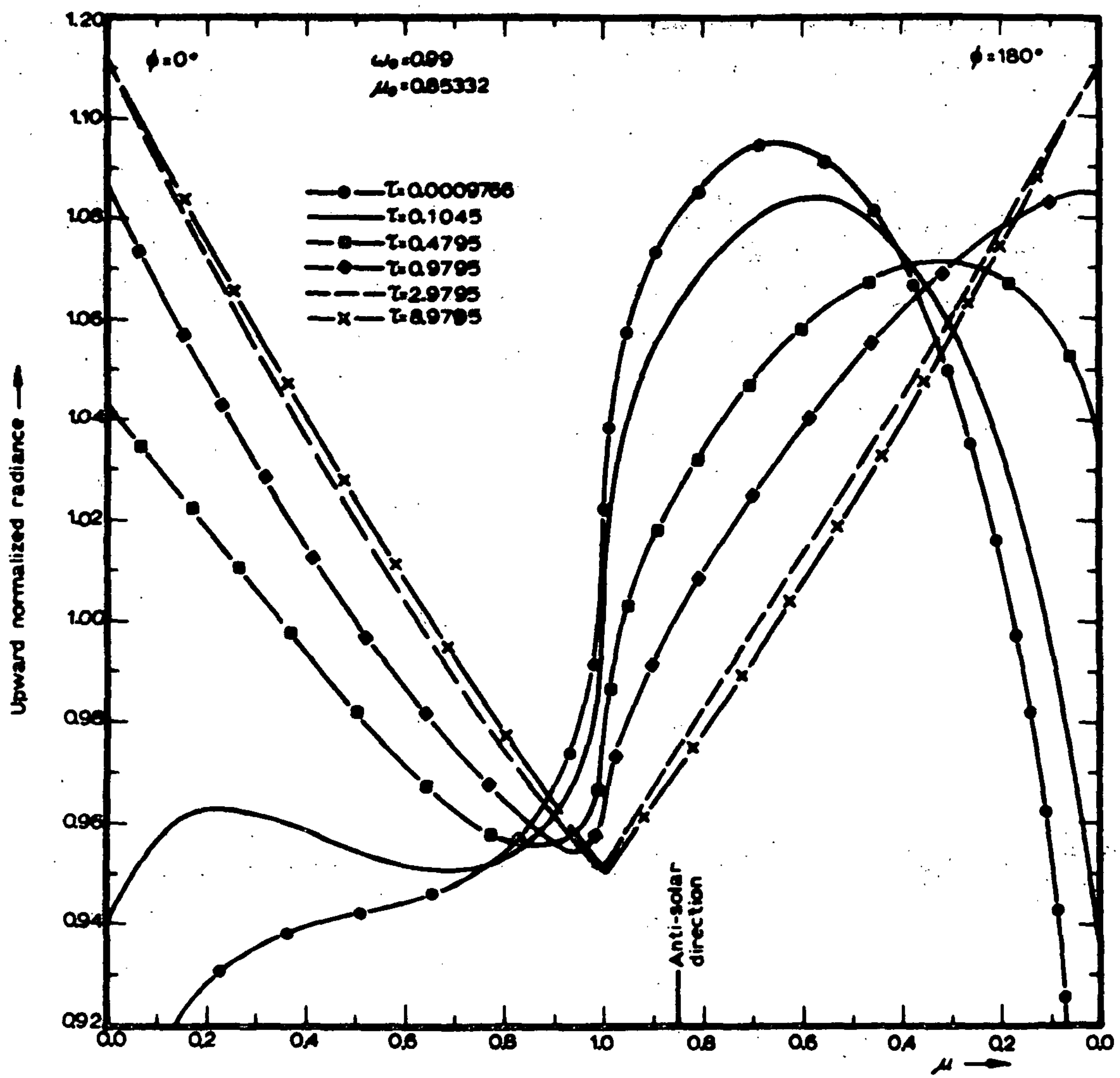

$\phi = 0°$
$\omega_0 = 0.99$
$\mu_0 = 0.85332$
$\phi = 180°$
$\tau = 0.0009766$
$\tau = 0.1045$
$\tau = 0.4795$
$\tau = 0.9795$
$\tau = 2.9795$
$\tau = 8.9795$
Upward normalized radiance
Anti-solar direction
μ
1.20
1.10
1.08
1.06
1.04
1.02
1.00
0.98
0.96
0.94
0.92
0.0
0.2
0.4
0.6
0.8
1.0
0.8
0.6
0.4
0.2
0.0

Fig. 7

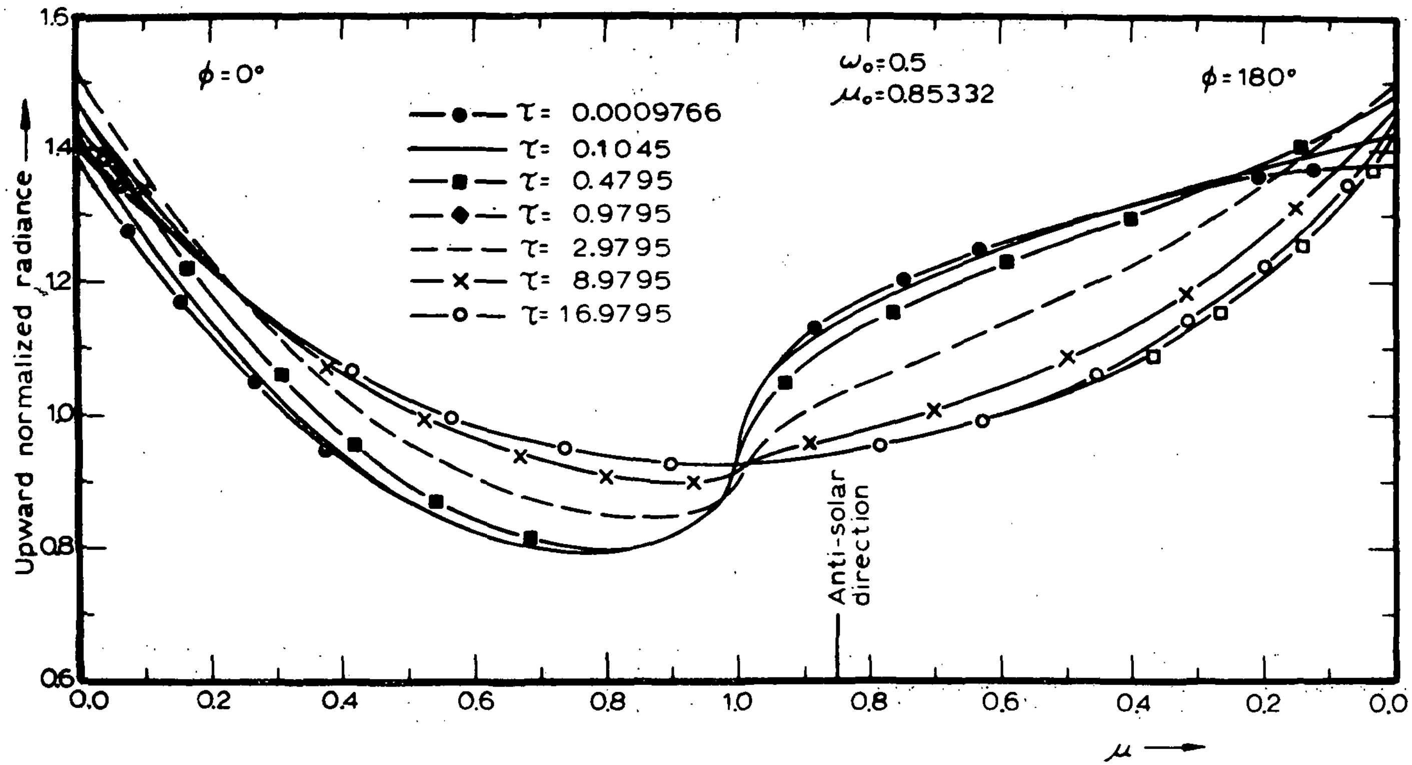

φ=0°
ω_o=0.5
μ_o=0.85332
φ=180°
τ= 0.0009766
τ= 0.1045
τ= 0.4795
τ= 0.9795
τ= 2.9795
τ= 8.9795
τ= 16.9795
Upward normalized radiance
Anti-solar direction
μ
1.6
1.4
1.2
1.0
0.8
0.6
0.0
0.2
0.4
0.6
0.8
1.0
0.8
0.6
0.4
0.2
0.0

Fig. 8

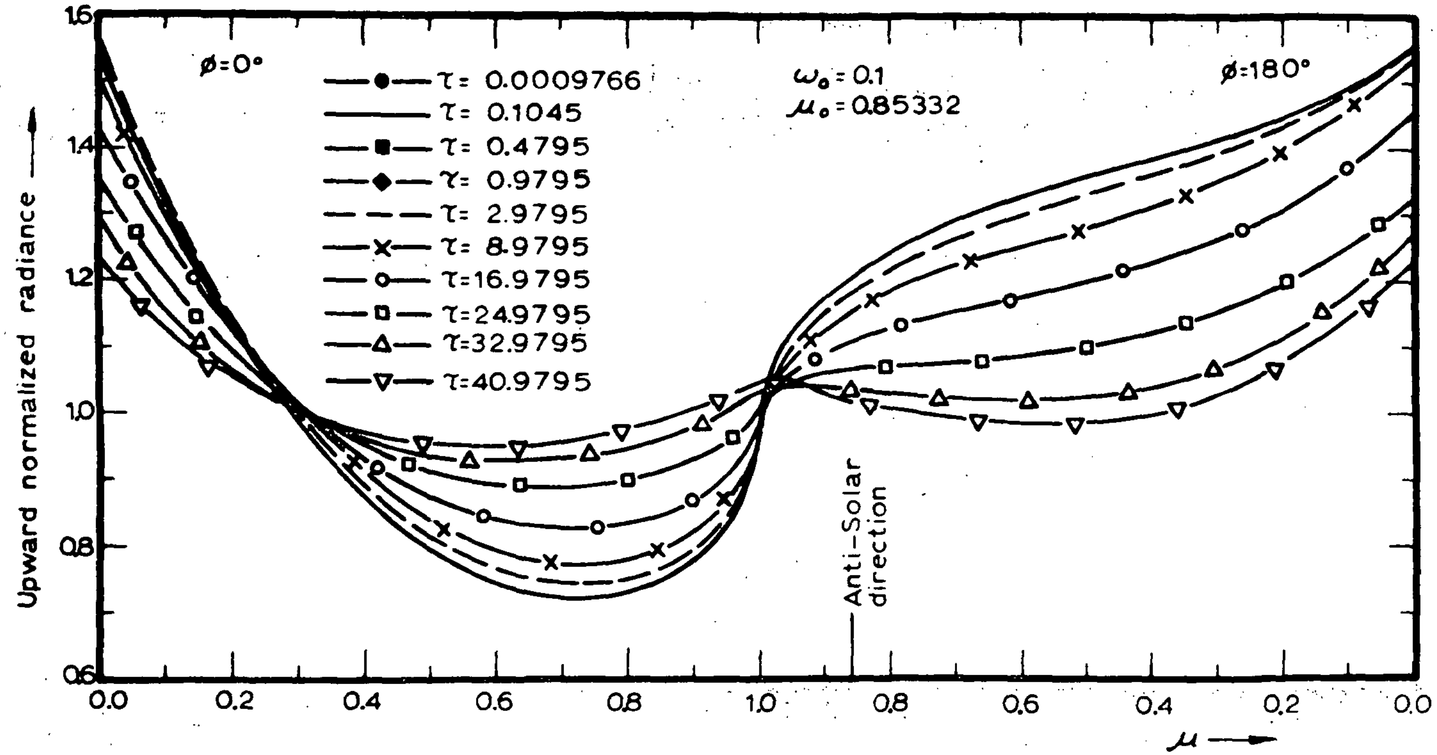
ø=0°
ø=180°
τ= 0.0009766
τ= 0.1045
τ= 0.4795
τ= 0.9795
τ= 2.9795
τ= 8.9795
τ=16.9795
τ=24.9795
τ=32.9795
τ=40.9795
ω₀= 0.1
μ₀= 0.85332
Anti-Solar direction
Upward normalized radiance
μ
1.6
1.4
1.2
1.0
0.8
0.6
0.0
0.2
0.4
0.6
0.8
1.0
0.8
0.6
0.4
0.2
0.0

Fig. 9

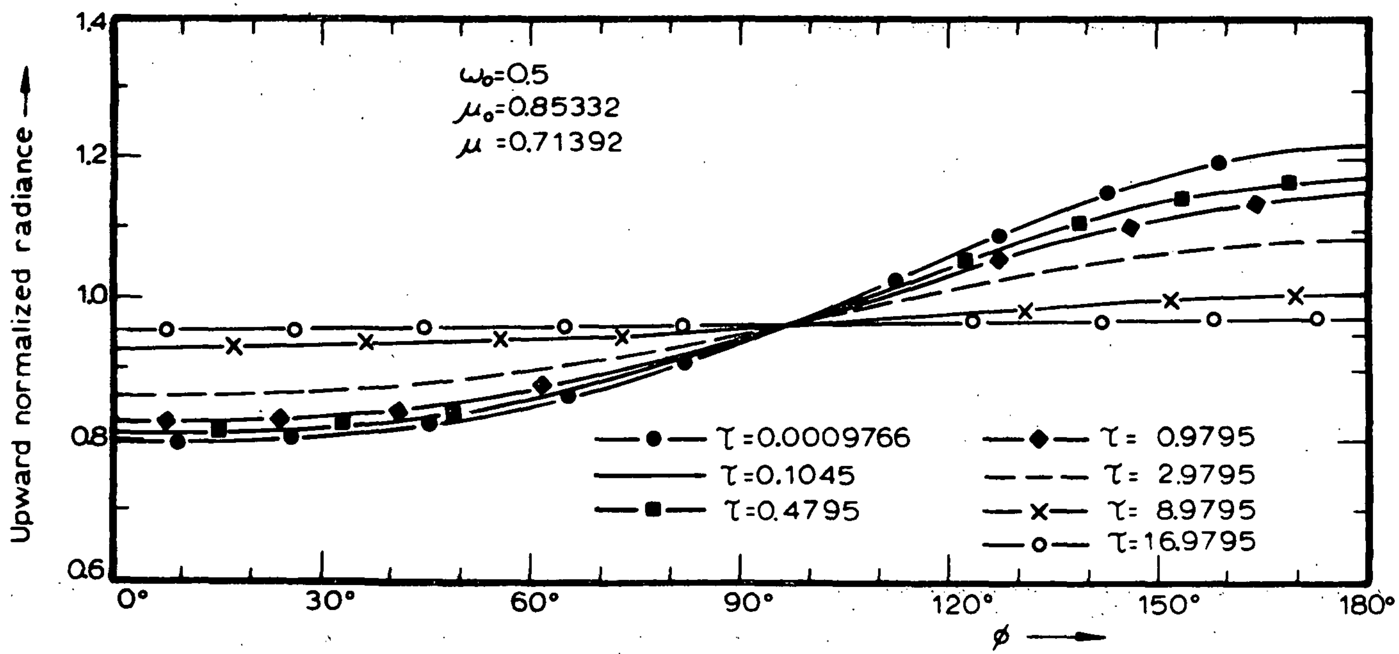

ω_0=0.5
μ_0=0.85332
μ =0.71392
τ=0.0009766
τ=0.1045
τ=0.4795
τ= 0.9795
τ= 2.9795
τ= 8.9795
τ=16.9795
Upward normalized radiance
1.4
1.2
1.0
0.8
0.6
0°
30°
60°
90°
120°
150°
180°
ϕ

Fig. 10

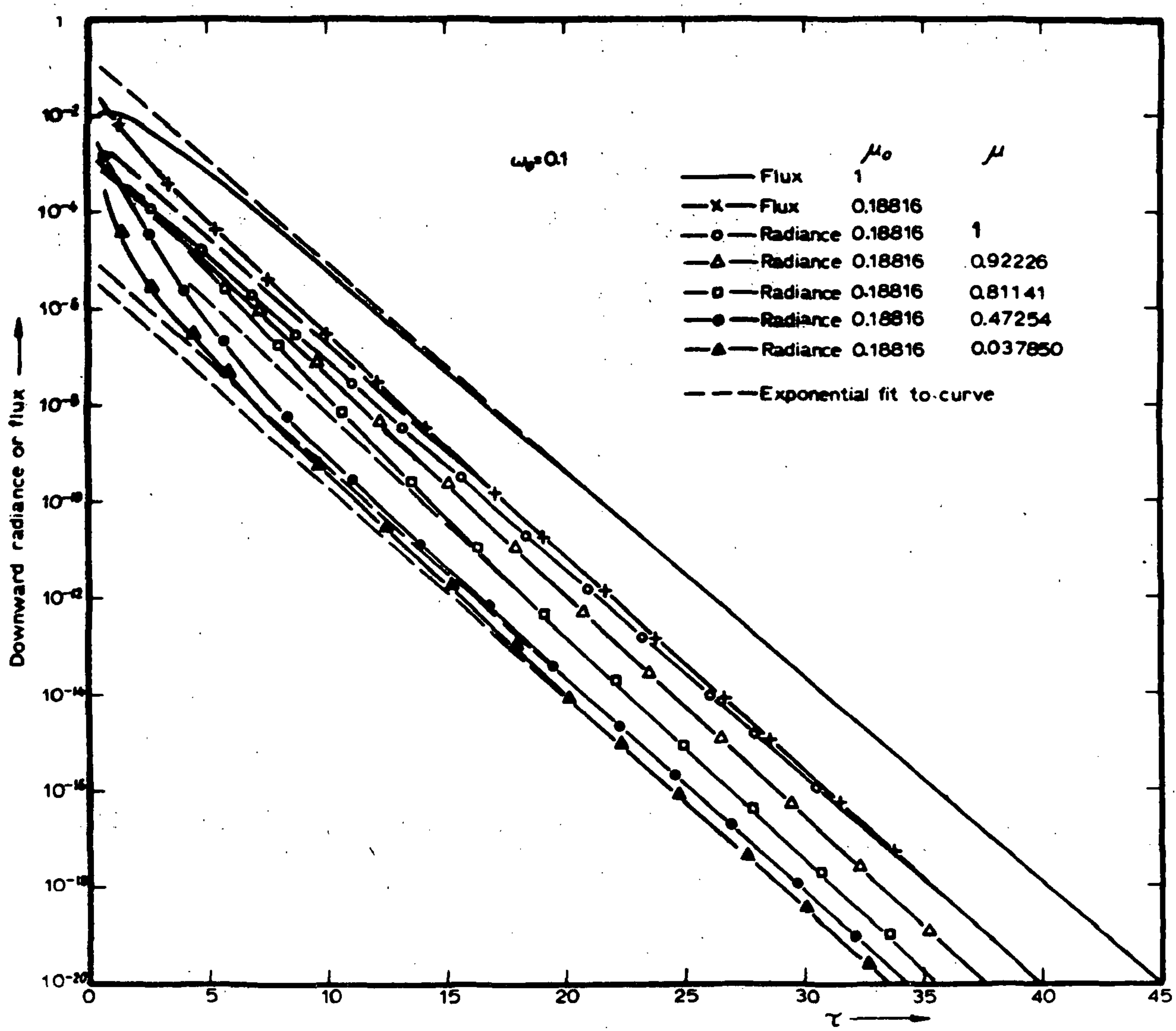

$\omega_0 = 0.1$
μ_0 μ
Flux 1
Flux 0.18816
Radiance 0.18816 1
Radiance 0.18816 0.92226
Radiance 0.18816 0.81141
Radiance 0.18816 0.47254
Radiance 0.18816 0.037850
Exponential fit to curve
Downward radiance or flux
τ
1
10^{-2}
10^{-4}
10^{-6}
10^{-8}
10^{-10}
10^{-12}
10^{-14}
10^{-16}
10^{-18}
10^{-20}
0
5
10
15
20
25
30
35
40
45

Fig. 11